applied sciences

MDPI

Article

Conductive Ink Printed Fabric Antenna with Aperture Feeding Technique

Philip Ayiku Dzagbletey and Jae-Young Chung *

Department of Electrical and Information Engineering, Seoul National University of Science and Technology, Nowon-gu, Seoul 01811, Republic of Korea
* Correspondence: jychung@seoultech.ac.kr

Featured Application: Wearable Antenna Technology.

Abstract: Screen-printed and inkjet-printed conductive fabric antennas have been investigated in this manuscript. The former showed optimal radiation performance after fabrication and measurement, which was the basis for developing a new fabric antenna feeding technique. The aperture-fed technique is achieved with a single coaxial cable overlayed on a cut-out slot on the ground layer of the patch antenna. The cable is connected with conductive silver-based epoxy paste with high resilience to mechanical stress. Two antenna models for Bluetooth low energy (BLE) and long-range (LoRa) wireless applications were designed, fabricated, and measured at 2.44 GHz and 868 MHz, respectively, with good impedance and radiation performance. The measured antennas operated from 2.4 to 2.48 GHz (BLE) and 853 to 886 MHz (LoRa) at −10 dB *S*11. Measured results also showed a 56% radiation efficiency at BLE and 44.9% at LoRa. The screen-printing procedure and feeding technique have been presented in this manuscript.

Keywords: antenna feeds; aperture-fed antennas; BLE; conductive textile; inkjet-printed antenna; LoRa; screen-printed antenna; wearable antennas

Citation: Dzagbletey, P.A.; Chung, J.-Y. Conductive Ink Printed Fabric Antenna with Aperture Feeding Technique. *Appl. Sci.* **2023**, *13*, 2902. https://doi.org/10.3390/app13052902

Academic Editor: Gang Lei

Received: 28 January 2023
Revised: 20 February 2023
Accepted: 21 February 2023
Published: 24 February 2023

1. Introduction

Flexible wearable devices have been at the center of recent smart clothing research as they can be easily integrated into regular clothing with minimal discomfort to the end-user; all the while maintaining the fashion aesthetics and intended communication capabilities. A 2020 in-depth analysis of recent advances in the wearable research industry [1] indicated that a critical concern in smart textile development is the elimination of on-body coupling while incorporating additional functionality to the antenna system. The others are the use of bendable, waterproof, and highly conductive fabric-based radiators.

In this regard, various research [2–8] has been conducted on material choice and manufacturing technologies to achieve highly conductive and functional fabrics. These technologies can be grouped into two general categories. First, is the use of conductive sheets or threads attached, woven, or embroidered into fabrics with differing meshing techniques. The second is the use of conductive inks and/or paint applied on fabrics using special screen-printing techniques. The former has been investigated by [5,6] and many others with the use of conductive yarns woven into radiating shapes such as a spiral or monopole. [7,8] developed wearable antennas by integrating fabrics with thin copper sheets shaped into radiator sizes for resonation. In addition to the obvious aesthetic discomfort to the wearer with the use of these solutions, these antenna technologies are difficult to integrate into existing clothing and pose a major challenge in input impedance matching. That is, the potential air gaps between the radiator and fabric substrates, irregular thread dimensions due to yarn coating, etc., result in unpredictable results.

Conductive ink applications [3,9,10], on the other hand, have overcome some of these challenges with the use of highly conductive inks such as silver base inks printed directly

(inkjet printing) on the target fabric or with the use of thin fabric bases such as polyester, cotton, or nylon which acts a conductive fabric bed. The latter technique, known as screen-printing, forms a thick quasi-conductive fabric that can be cut into various radiator shapes and integrated into the target fabric. Both of these techniques will be investigated in this letter to obtain performance characteristics, similar to what is presented in [3].

After choosing a suitable conductive ink technique, another major challenge with textile antenna integration is feeding. The widely used method of exciting the printed and/or woven antenna is with a SubMiniature version A (SMA) probe or edge feeding as implemented in [3,4,9] among others. Although very excellent radiation and return losses are obtained, the bulkiness of the SMA connector inhibits the general adaption of these antennas into mainstream clothing.

To this end, as shown in Figure 1, simple patch antennas have been developed and presented in this paper to show progressive advancements in the field of flexible, on-body compatible antennas using ordinary fabric textiles. An in-house, silver-ink screen-printed polyester base conductive fabric has been developed with high conductivity, high stretching, and bending resistance with the screen-printing technique [4]. The antennas (shown as model #1, #2 and #3) were developed at 2.44 GHz and 868 MHz, which are widely used frequency bands for long-range communication. Bluetooth low energy (BLE) operating at 2.4 to 2.48 GHz and long-range wireless access networks (LoRaWAN) operating at 863 to 870 MHz are some of the popular communication standards used in long-range track and detection, Internet of Things (IoT) communication devices, etc.

Figure 1. Illustrated view of fabric-based antennas integrated into fabric clothing.

Additionally, a coaxial feeding technique has been developed and tested at these LoRa and BLE frequency bands. The feeding technique is a proximity-fed aperture coupling of the radiating patch with a coaxial cable attached to the ground plane. The effectiveness of the technique in replacing dielectric resonating reflectors in mitigating large back radiations associated with aperture-coupled patch antennas has been proven with measured results using conductive screen-printed antennas.

This research aims to develop practical and high-performing antennas at a commercial level with seamless integration into everyday clothing with little or no discomfort to the wearer. The authors believe this to be a step in the right direction for smart clothing technology.

Section 2 elaborates on the materials used and the distinction between the use of ink-jet/direct printing and screen-printing techniques. Section 3 describes the antenna design and measured results of the direct printed and screen-printed techniques. Section 4 introduces the aperture-coupled cable feeding technique. This antenna feeding method, the first of its kind to be used on fabric antennas, was tested with a patch antenna and measured results have been presented as well.

2. Material Selection and Pre-Processing

Generally, fabric-based antenna research focuses mainly on the ergonomic and electrical properties of fabric materials. An essential aspect of antenna development is the selection and/or fabrication of the materials that constitute the antenna. The electrical and mechanical properties of these materials are of utmost importance as they determine to a large extent, the radiation performance of the antenna. Such materials include the fabric type to be used for the radiators and ground layers, substrates or spacers, conductive yarns and inks, adhesive films, conductive glue or epoxy, and cabling.

For the purpose of this research, the target fabric refers to the textile-based material into which the final antenna will be integrated. This will act as the dielectric substrate on which a conductive ink layer will be dispensed or printed on its top and bottom layers to create a microstrip structure. The base fabric thus refers to a thin fabric material on which conductive ink is soaking in, dispensed, or printed to be used as a conductive sheet that can be cut into any planar shape.

2.1. Base Fabric Materials

There is no base fabric for the direct printed antennas since the conductive inks are directly applied to the target fabric. However, for screen printing, several considerations were undertaken in the choice of base fabric materials to use. One such consideration is the ink absorption of the base fabric which is directly related to the yarn-weaving technique and a fabric pre-processing called calendering. Yarns with a flat cross-sectional area (flat yarns) were reported in our previous findings in [4] to be superior in absorbing silver-based inks better than round yarns (yarns with a rounded cross-section). In addition, the calendering process of compressing the fabric through heated rollers offers the flat yarns a smoother and even surface roughness (after ink application) compared to round yarns. Surface roughness is a key characteristic that determines the conductivity of a material [11]. Other considerations for the base fabric include the ability to withstand mechanical stress, ease of production, and availability as well as stretchability.

The base material used for the screen printing was thus flat yarn-based polyethylene terephthalate (PET) fabric or polyester as it met most of the mechanical, economical, and electrical properties suitable for ink absorption and mass printing.

2.2. Screen-Printing of Conductive Ink

This technique is widely known in the textile printing industry as it affords large-scale printing and fast production on an economic scale. It is achieved by pressing conductive ink over a meshed screen onto the base fabric which can therefore achieve high print resolution and uniform electrical conductivity based on several factors. The screen mesh size, the number of print cycles, screening speed, the viscosity of conductive ink, as well as the curing procedure, are some factors that determine the outcome of the print quality [12–14].

After careful research into these findings and our investigations presented in [4,9], the screen-printing properties used were 70-mesh openings per 1 inch (pixel/in) with each opening being $\approx 280 \times 280$ μm^2 and mesh wire diameter of ≈ 75 μm. A high mesh resolution however offered better surface roughness with less viscous conductive ink. Using a silver-based conductive ink (Electrodag 479SS) from Henkel Co. [15] which has a viscosity of 12,000 mPas(cP) and sheet resistivity of 0.02 Ω/sq/mil, the ink's bulk conductivity was deduced at 1.97 MS/m (bulk conductivity of copper = 58.7 MS/m).

Although lower than copper, this value was high enough to achieve comparable gain performance as shown in [9]. The course silver particles present in the Electrodag 479SS ink or paste makes it more conductive and thus more viscous.

With this high viscosity, a lower resolution mesh of 70 pixels/inch will perform better than a higher resolution as a highly viscous ink paste permeates a wider aperture mesh more evenly. The number of printing layers was also limited to two as presented in [3] and [4] to be the best number for screen-printed conductive fabrics. These however also depend on several factors such as the mesh size, curing time, and ink viscosity among others. Printing more than two layers on the 70 pixel/in mesh did not increase the electrical performance of the conductive fabric [4]. The final material takes about 24 to 48 h to completely cure and be ready for use as a conductive textile sheet.

3. Antenna Design

3.1. Simulation and Fabrication

The antennas were first designed and simulated in ANSYS Electronics Desktop [16] and then fabricated and measured. Figure 2 shows a prototype of the fabricated antennas and SMA integration concepts for direct and inkjet-printed fabric antennas. A simple square patch antenna is designed to obtain a comparative performance analysis of the two printing techniques at 2.4 GHz. That is the direct/inkjet print method and screen printing.

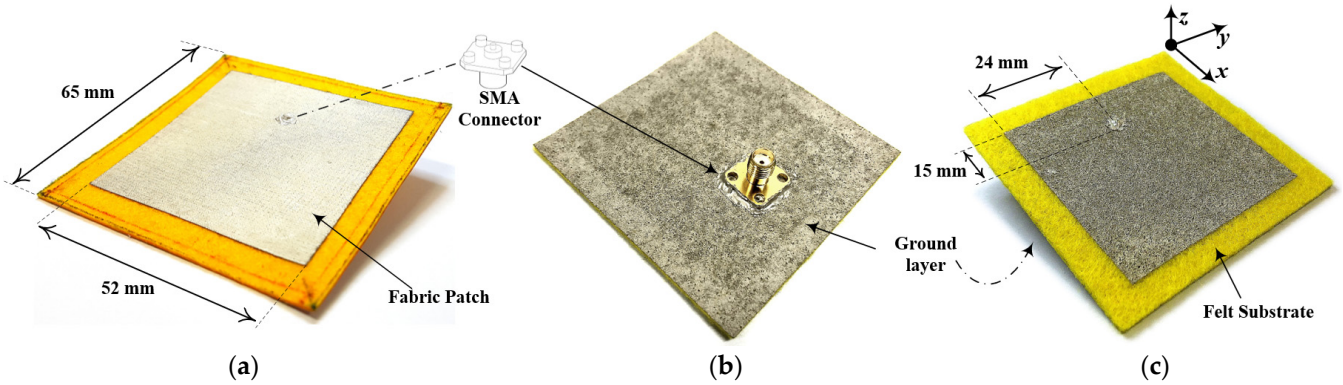

Figure 2. Fabricated antennas showing (**a**) top view of probe-fed patch antenna with conductive polyester base fabric, (**b**) back view of direct printed probe-fed antenna showing SMA attachment (**c**) top view probe-fed antenna with direct printed silver ink.

The base fabric from the screen printing (polyethylene terephthalate (PET)), is now a conductive fabric sheet measuring 0.12 mm in thickness. This was used for the radiator and ground layer of the patch antenna in Figure 2a. The probe-fed patch antenna is designed with specifications from [17]. The square-shaped radiating patch measures 52 mm on either side. The same material is used for the ground layer which is attached to a 66 mm^2 felt substrate. A 10-micrometer adhesive film bonds the 0.12 mm polyester patch and ground with the 1.0 mm thick substrate. To eliminate and/or minimize geometrical errors, a specialized cutting tool was obtained from Cricut Inc. (Maker 3®) for cutting all fabric materials and adhesive tapes.

A thin substrate of 1 mm was used to demonstrate a worst-case scenario for a lossy felt substrate. As with all probe-fed patch antennas, the SMA connector is attached to the patch and ground layers using conductive epoxy paste with high silver concentration and fast curing time. The resulting antenna shown in Figure 2a is mildly heated and pressed to ensure maximum bonding of the layers.

Similarly, the direct printed antenna was designed and fabricated by directly injecting and printing the silver ink on a pre-treated felt fabric. The pre-treatment involved thermal pressing at 150 degrees Celsius to ensure an even surface to maximize ink adhesion. The Mateprincs SCAG-003 [18] silver–copper-based conductive ink was used with a viscosity of 14,550 mPas and sheet resistivity of 0.05 mΩcm (0.025 mΩ/sq), thus achieving bulk conductivity of 0.04 MS/m. The ground plane was printed first and cured at 130 degrees Celsius for 5 min, and then the radiating patch was also printed and cured for the same duration. The direct print resulted in a thicker conductive layer of 0.35 mm compared to the screen-printed method which achieved 0.12 mm thickness. The fabricated model is shown in Figure 2b,c.

As explained earlier with the differences in the two printing techniques, it was not feasible to use the same inks for the two methods as their printing mechanisms and ink viscosity requirement were different. In addition, to ensure optimum results for each technique, it was necessary to use the best available conductive ink that is optimal for each printing method.

From Figure 2, each antenna measured 66 mm^2 with a patch size of 52 mm^2. The thicknesses of the antennas were 1.24 mm and 1.7 mm for screen-printed and direct printed methods, respectively. The SMA connector added an extra thickness of 9.5 mm (SMA receptacle length) to both antenna models.

3.2. Measurement

Figures 3–6 show the simulated and measured results of the two printing techniques with a summary comparison shown in Table 1. The measurements were performed with both a vector network analyzer and in an anechoic chamber to verify the electrical performance of the antennas. The radiation efficiency is a measured ratio of the total radiated power of the antenna in a 3D sphere with the input power at a given frequency point. (center frequency).

Table 1. Comparison of direct/inkjet printing vs. screen-printing of fabric patch antenna.

	Conductive Ink	Bulk Conductivity (MS/m)	Antenna Size (Length × Width)	Measured Bandwidth (GHz)	Measured Gain (dBi)	Rad. Eff. (η_{eff})	FBR (dB)
Screen-printed	Electrodag 479SS	1.97	66 × 66 × 1.24	2.37–2.44 (70 MHz)	6.77	59.72	7.08
Direct/inkjet printed	Mateprincs SCAG-003	0.04	66 × 66 × 1.70	2.39–2.46 (70 MHz)	4.66	44.31	10.76
Copper-sheet on felt fabric	Copper sheet	58.7	65 × 65 × 1.06	2.36–2.42 (60 MHz)	7.57	83.79	9.61

patch antenna sizes without SMA connector. | Rad Eff. = radiation efficiency | FBR is front-to-back ratio.

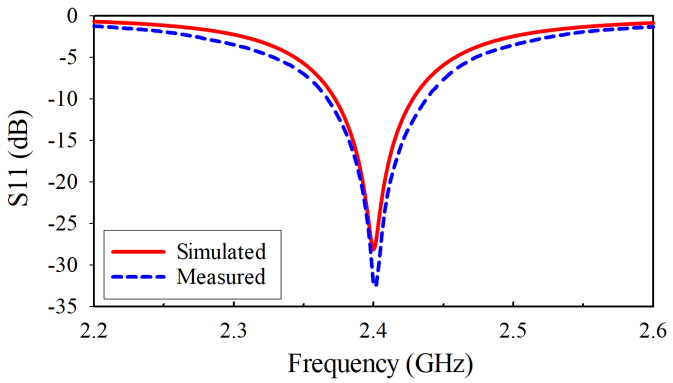

Figure 3. *S*11 curve of screen-printed antenna.

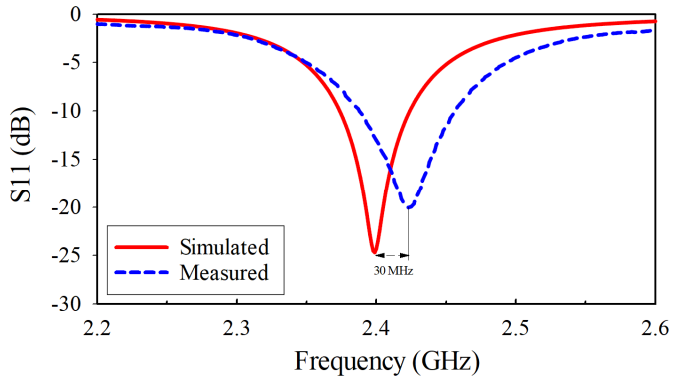

Figure 4. *S*11 curve of direct ink-printed antenna.

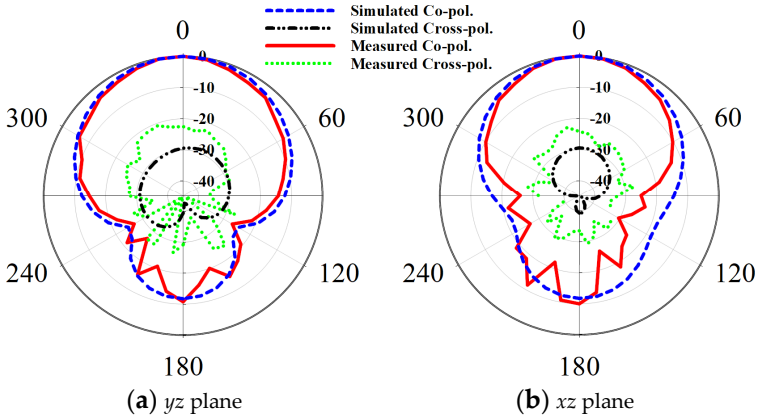

Figure 5. Normalized radiation patterns of screen-printed antenna at 2.4 GHz.

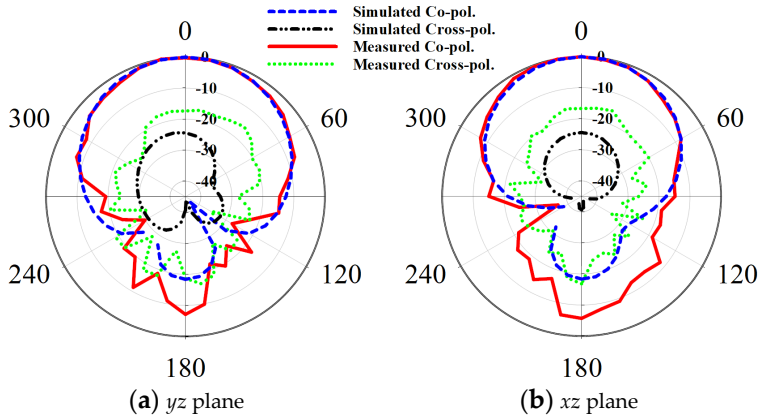

Figure 6. Normalized radiation patterns of direct ink-printed antenna at 2.4 GHz.

From Figure 3, the screen-printed antenna obtained a simulated bandwidth of 2.37 to 2.43 GHz (60 MHz) and a measured range of 2.37 to 2.44 GHz (70 MHz) at −10 dB S11. Although the simulated and measured reflection coefficients (*S*11) results were similar, the radiation patterns recorded differing gains of 4.17 dBi and 6.77 dBi at 2.4 GHz for simulated and measured, respectively. This can be attributed to incorrect simulation values for the bulk conductivity of the base fabric (conductive PET). The radiation pattern in Figure 5 nonetheless shows conformal patterns in both the simulated and measured results with cross-polarization values lower than −20 dB.

Figure 4 shows the reflection coefficient of the direct printed method with a visible shift in the simulated bandwidth compared to the measured. Simulated $S11$ at -10 dB is observed from 2.38 to 2.42 GHz (40 MHz bandwidth) and for measured $S11$ from 2.39 to 2.46 GHz (70 MHz). In addition to incorrect bulk conductivity approximations, the difference could be attributed to fabrication errors with the epoxy application, SMA pin misalignment, and poor curing of epoxy resin.

The radiation pattern shown in Figure 6 recorded a 3.4 dBi simulated gain and a 4.66 dBi measured gain at 2.4 GHz. The measured front-to-back ratio (FBR) of the direct printed antenna indicates large back radiation which can be attributed to the uneven nature of the printed ground plane resulting in an increased surface current and also fringing effects from the thick 0.35 mm conductive ink layer.

The comparison in Table 1 shows a better performance of the screen-printed fabric antenna over the direct printed. Although the poorly measured gain of 4.66 dBi can be attributed to the low bulk conductivity, the printing technology could not permit the use of a denser conductive ink without clogging the nozzle of the printer. The table also shows a similarly designed probe-fed patch antenna with 0.05 mm thin copper film on a 1 mm felt substrate. This was designed as an ideal reference for the two printing methods. As can be seen, with a bulk conductivity of 58.7 MS/m, the copper-based variant obtained a radiation efficiency of 83.79%, and a measured gain of 7.57 dBi but with a narrower bandwidth. It is thus important to note the comparable performance of the screen-printed fabric patch antenna with the reference copper model with respect to the realized antenna gain, radiation efficiency, and front-to-back ratio. With just a 24% drop in radiation efficiency compared with the copper model, the conductive PET can replace a copper sheet and achieve comparable results.

Following the successful verification of the screen-printed fabric antenna as being superior to the ink-jet-printed antenna and electrically comparable with the copper-based model, the next section will focus on developing a new feeding mechanism that eliminates the use of an SMA directly on the fabric antenna. The antenna in Figure 2a and the results in Table 1 will thus serve as benchmarks in determining the performance of this feeding approach.

4. Antenna Feeding for Fabric Antennas

As illustrated in the previous section and by most fabric-based antenna research, the SMA port connection either by probe or edge feeding [19] is the commonest method to feed the fabric patch antenna and achieves somewhat of an ideal performance without any real-world application intended. In that respect, to properly and efficiently achieve smart clothing applications, the ergonomic features of the antenna must be taken into consideration. Alternate feeding methods include a stripline approach that feeds the radiators directly with a printed stripline, with the obvious drawback being spurious surface current induced between the ground and the radiator on the same plane.

The third and less common method is the aperture feeding technique using dielectric-induced resonators and/or reflectors. This technique provides a slight advantage over the conventional SMA ports and the stripline methods but with a high level of complexity and antenna thickness making it unattractive. For instance, the most recent design iteration reported in [20–22] shows a five-layer antenna with the first part comprising the patch, substrate, and ground with an aperture slot. This first part is entirely fabric based. Attached to the ground is the second part, made of printed circuit board (PCB) feed isolator/substrate and microstrip line (on the PCB backside) with a soldered coaxial cable.

The currents flowing through the microstrip line is induced onto the ground aperture, designed to resonate at certain wavelengths to feed the top patch. Although not a truly fabric-based solution with the inclusion of the PCB, miniaturization techniques in [20] enable the second part to be small compared to the antenna size. This method also provides wider bandwidths in certain cases. However, the risk of failure becomes high as special care is required to solder and/or attach the PCB to the fabric ground layer without burning the cloth while minimizing the air gaps that can potentially result in impedance mismatches. In addition, the PCB inclusion presents a similar ergonomic discomfort to the cloth end-user as both PCB and SMA poke into the undergarment.

In this section, the authors experimented with the aperture feeding technique but implemented it in a unique way to suit printed fabric antennas with minimal discomfort.

4.1. Aperture-Coupled Feeding with Coaxial Line

Figure 7 shows the conceptual views of the feeding technique with a coaxial cable mounted on a fabric patch antenna. Two antenna models are designed with the feeding technique at BLE and LoRa frequency bands. As stated in Section I, both technologies are ideal for long-range on-body mobile communication with low energy consumption support for IoT devices.

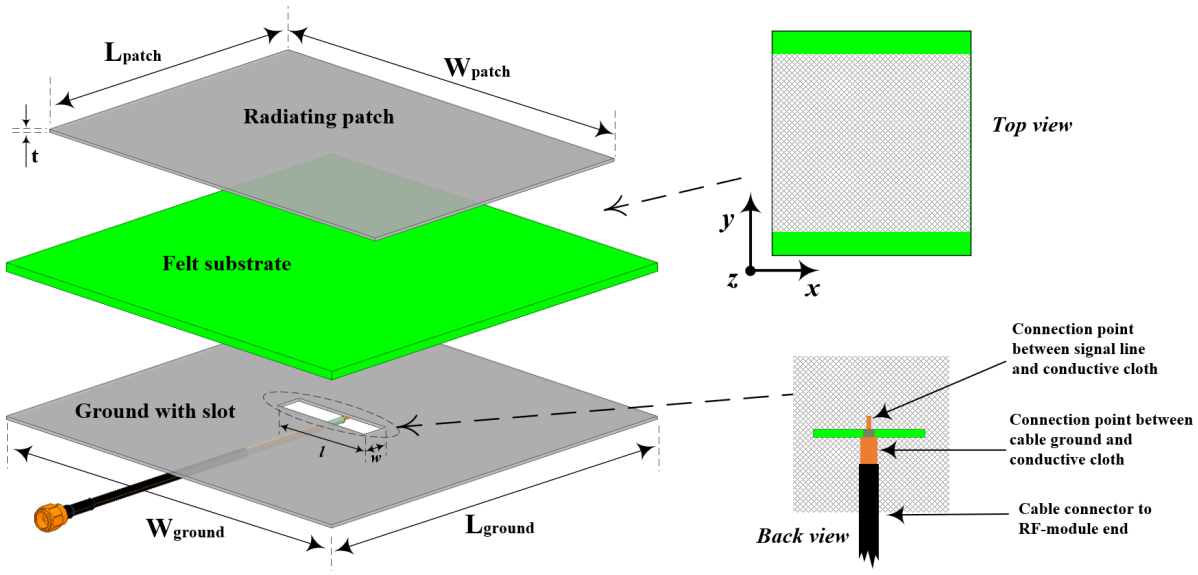

Figure 7. Conceptual views of the coaxial aperture-feeding technique (see Table 2 for dimensions).

Similar to a regular patch antenna, a 3 mm felt fabric (εr = 1.36, tan δ = 0.02.) is sandwiched between the radiating patch and ground layers, which are both made from conductive printed fabric, elaborated in Section II-B. The aperture slot splits the ground layer into two alternating sections when current is applied to the cable, enabling the aperture to act as a resonating electromagnetic gap at the given frequency of operation. In this regard, the aperture length (l) is approximately $\lambda g/4$ ($\approx$72 mm @ 868 MHz/$\approx$ 26 mm @ 2.44 GHz), thus making the aperture a quarter-wave dipole slot with maximum voltage amplitude at either end of the aperture. The narrow slot creates a high impedance traveling current towards the aperture ends. This phenomenon in turn drives the current upwards to the low impedance radiating patch, hence the coupling. When performed optimally, this technique results in lower back lobe radiation, which is a critical drawback to the aperture feeding method.

Unlike traditional patch antennas, the radiating patch width (*Wpatch*) shown in Figure 7 is optimized to the same width as the ground width (*Wground*). This is performed to ensure optimum coupling from the end sections of the aperture slot to the radiating patch. In this instance, a trade-off is made between maximum coupling for back lobe reduction and fringing currents required for the *yz* plane radiation pattern. Fringing currents at the patch edges (*yz* plane) are optimized with the use of the thicker 3 mm substrate and an optimized slot length. The patch lengths are optimized at λg/2 of the operating center frequency. Table 2 shows the optimized parameters.

Table 2. Parameter List for Aperture-Fed Antenna.

Parameters	BLE Model (mm)	LoRa Model (mm)
Lpatch	43	125
Wpatch	42	145
Lground	52	150
Wground	42	145
w	1.0	1.2
l	25.5	72
t	0.24	0.24

4.2. Fabrication

The stable impedance at the feeding section is maintained on the aperture by carefully placing the dielectric section of the cable on the aperture slot with equal widths. The signal wire mesh is fixed to the upper section of the ground (above the slot) while the cable ground mesh is fixed on the lower section as shown in Figure 7. The exposed cables are fixed to the conductive fabric using conductive epoxy with a high curing/adhesion property. After 24 h of curing, the backside is shielded with a low loss of 0.1 mm polytetrafluoroethylene (PTFE) silicone adhesive tape [23]. The resulting antenna is shown in Figure 8a,b, revealing the cable placement with cured epoxy. The assembly of the radiating patch and ground follows the same procedure used in Section III-A.

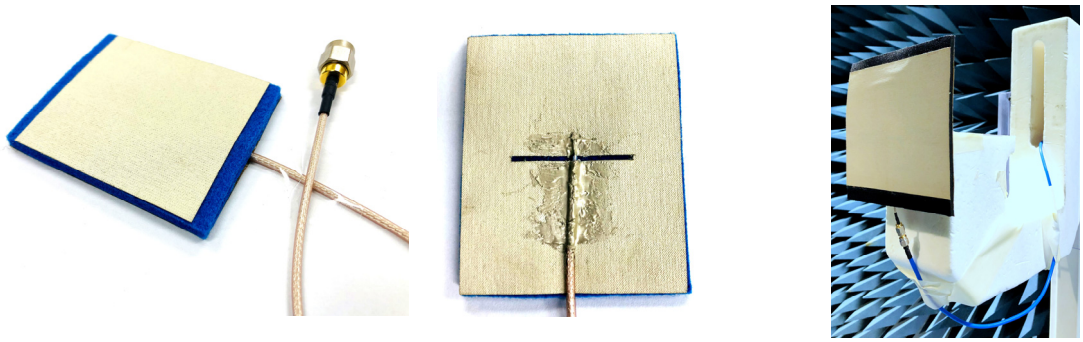

(**a**) Front view (BLE) (**b**) Back view (BLE) (**c**) Chamber measurement of LoRa model

Figure 8. Photos of fabricated BLE antenna model.

5. Measurement and Result Discussion

The fabricated antenna models (BLE ad LoRa) are measured to validate the aperture-coupled feed technique with coaxial cable and that of the modified patch structure. Figure 8c shows the anechoic chamber setup for the LoRa antenna model. The results presented in Figures 9–12 show excellent gain and return loss performance, nearing that of a regular PCB microstrip patch. Figures 9 and 10 show the simulated and measured *S*11 of the BLE and LoRa models, respectively. With a measured impedance bandwidth of 82 MHz (2.40–2.482 GHz) at −10 dB *S*11 shown in Figure 9, the measured BLE model operates well within the 2.44 GHz band. The LoRa model result shown in Figure 10 is measured at −10 dB *S*11 from 853–885.5 MHz, representing 32.5 MHz bandwidth, also operating within the LoRa band. Both models are comparable to the simulated results with minimal differences.

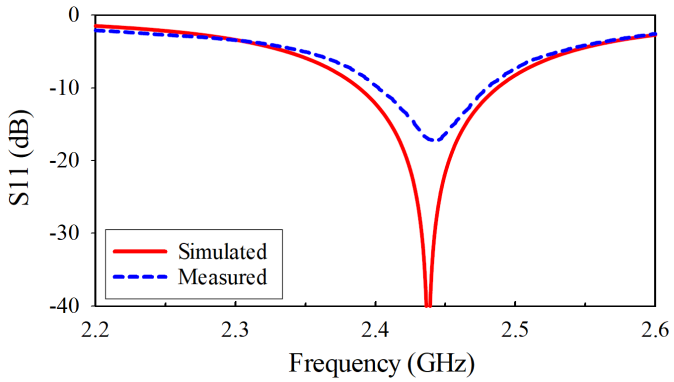

Figure 9. *S*11 curve of BLE aperture-fed antenna (2.44 GHz center frequency).

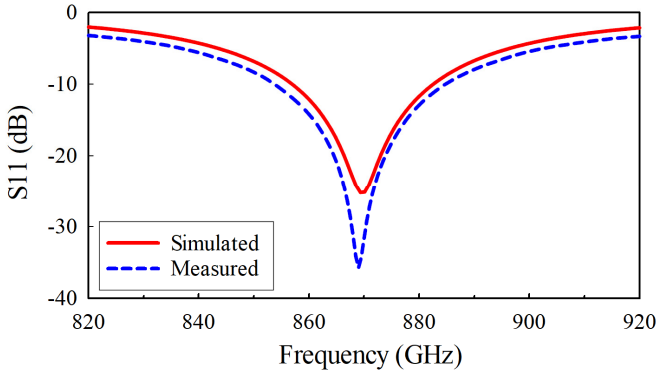

Figure 10. *S*11 curve of LoRa aperture-fed antenna (868 MHz center frequency).

The success of the correlating results was a result of using very precise cutting tools, minimal epoxy application, and low-loss adhesive film. The conductive epoxy adhesive can significantly affect the impedance performance when not applied and cured properly. Figure 10, for instance, shows slightly improved results in the *S*11 of the measured data compared with the simulated. This among other reasons stated already may also be due to the marginal inaccuracies of representing the dielectric coefficient, conductivity, and loss tangents of the newly created conductive materials used in these models. Further discussions on this are shown in [4,9].

Figures 11 and 12 show the normalized radiation patterns in the *yz* and *xz* planes of the BLE and LoRa models, respectively. A measured antenna gain of 3.85 dBi at 56.1% radiation efficiency (η_{eff}) is recorded at 2.44 GHz. The simulated gain was obtained at 5.1 dB, representing a 1.25 dB drop in measured gain. A front-to-back (FBR) of better than 9.35 dB (≈−5.5 dB back radiation) is recorded in both planes and HPBW of 78.8 deg. and 73.76 deg. is recorded in the *yz* and *xz* planes, respectively.

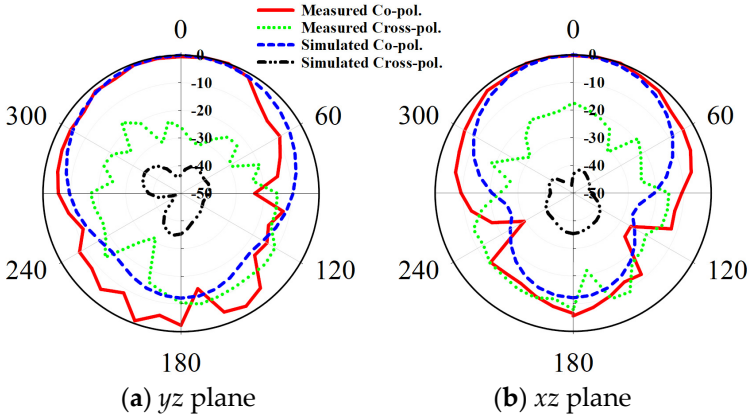

(**a**) *yz* plane (**b**) *xz* plane

Figure 11. Normalized radiation patterns of aperture-fed antenna (2.44 GHz).

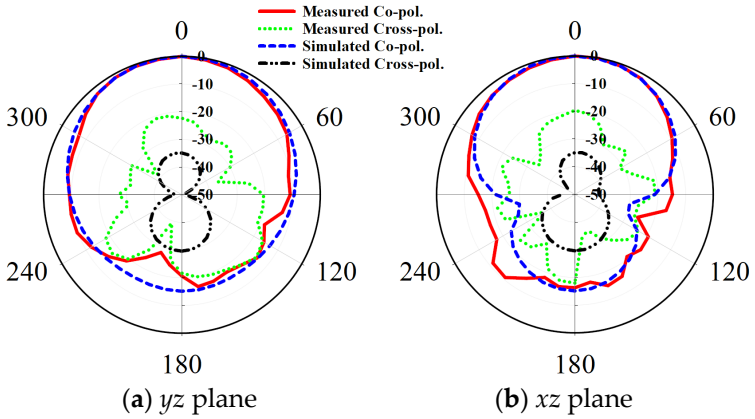

(**a**) *yz* plane (**b**) *xz* plane

Figure 12. Normalized radiation patterns of aperture-fed antenna (868 MHz).

With the LoRa model, an antenna gain of 3.9 dBi is measured at 868 MHz with η_{eff} of 44.92%. The simulated gain was obtained at 3.5 dB. A front-to-back (FBR) of better than 20.62 dB (≈−16.7 dB back radiation) is recorded in both planes. Measured HPBW is observed at 87.6 deg. and 73.4 deg. for *yz* and *xz* planes, respectively.

The BLE model in particular resulted in an FBR of 9.35 dB compared with the LoRa with 20.62 dB. Although comparable to some aperture-coupled antenna results shown in Table 3, this may be attributed to the higher fringing radiations in the *yz* plane resulting in increased surface currents on the ground plane. The smaller patch size of the BLE model thus resulted in a larger back lobe radiation. This can be corrected by increasing the ground size of the antenna and/or the substrate thickness. Conversely, the minimized back lobe observed in the LoRa model shows the performance improvement of this feeding technique over the traditional aperture-fed patch antenna with suppressed back lobe.

Table 3. Comparison of fabric-based patch antennas with aperture/proximity feeding techniques.

Ref.	Aperture Feeding Technique	Antenna Size * L × W × H (mm)	Bandwidth (GHz)	Fractional Bandwidth	Gain (dBi)	Rad. Eff. (η_{eff}) **	FBR. (dBi)
[19]	Proximity feed with probe	50 × 50 × 4.0	2.36–2.51	6.16%	1.5	55%	-
[20]	Dielectric back-reflector	100 × 100 × 4.8	2.33–2.49	6.63%	5.6	47%	15
[21]	Dielectric back-reflector	40 × 60 × 1.03	2.39–2.49	4.1%	-	58%	-
[22]	PCB solar cell reflector	120 × 120 × 11.95	0.902–0.928	2.84%	3.0	-	4.0
[24]	SMA side-feed with AMC back-reflector	68 × 68 × 4.5	2.0–2.6	26.01%	2.86	65%	-
Proposed designs (coaxial cable with epoxy resin)		52 × 42 × 3.24	2.4–2.482	3.36	3.85	56%	9.35
		150 × 145 × 3.24	0.853–0.886	3.73	3.9	44.92%	20.62

* L × W × H = length × width × height | ** Rad Eff. = radiation efficiency | fractional bandwidth is at −10 dB S11.

The cable placement on the antenna ground layer had minimal effect on the radiation pattern. However, some distortions in the pattern can be observed especially in the *xz* plane of the LoRa model and both planes of the BLE. The patterns show a dip between theta 90 to 120 degrees which is the plane on which the cable is laid. An effective suggestion might be to use thinner cables with a higher grade of shielding; both of which were expensive and inaccessible to the researchers in the course of the design.

Another area of concern was the cross-polarization (x-pol.) values obtained in the measured results of the BLE model. The measured x-pol. values towards the back-end of the model were rather high as seen in Figure 11a,b. A −5.1 dB x-pol. value in the *xz* plane and −7.7 dB in *yz*. Similar to the back radiation, this could be attributed to the smaller ground size which resulted in spurious fringing currents not being properly grounded. The occurrence is not observed in the LoRa model with a 150 × 145 ground size, achieving x-pol. values better than −13.9 dB and −17.7 dB in the *xz* and *yz* planes, respectively.

Although lower, the radiation efficiency of the aperture-coupled fabric antenna is comparable to the reference copper sheet-based felt patch antenna at 84% radiation efficiency (see Table 1) with the former having a bulk conductivity of 1.97 MS/m and copper being 58.7 MS/m. (97% difference). The measured antennas performed well in the measurement with good conformity with the simulation in general.

Recent fabric-based antennas with aperture/proximity feeding techniques are shown in Table 3 and compared with the proposed design. As shown, the aperture-coupled antenna with coaxial cable feed performs comparatively well to the referenced works with respect to the parameters shown. Reference [22] showed a PCB-backed solar cell placed on a thick 11.95 mm fabric that operated in the North American LoRa frequency band of 915 MHz. Although it obtained a good single element gain value of 3.0 dBi at a 2.84% fractional bandwidth, the front-to-back ratio was very poor owing mainly to the aperture slot method used. An improved concept is observed in [19–21] with radiation efficiencies close to the proposed designs. The SMA probe-fed design in [24] produced a very good radiation efficiency value of 65% from an initial low of 10% due to the inclusion of the artificial magnetic conductor (AMC) backed reflector. However, as mentioned earlier, the PCB components in these feeding structures make the antenna generally bulky with little comfort when worn due to the inflexible PCB back structure. In addition, the back reflectors are added primarily to mitigate the large back radiations in the aperture feeding structures [21]. The proposed design achieves comparable front-to-back ratios and radiation efficiencies as shown in Table 3 without the need for back reflectors and inflexible PCB structures. The objectives set out in this manuscript in finding a suitable and simple solution to feed fabric antennas were thus achieved.

6. Conclusions

Screen printing and direct/inkjet printing of conductive fabric technologies have been studied in this manuscript with the former showing better performance with fabricated and measured samples. The screen-printed antennas were further used in developing an aperture-coupled coaxial feeding technique that aimed at providing a simple and practical feeding method for fabric antennas. The technique enables the complete elimination of SMA connectors and PCB back reflectors used in most fabric antenna development, thus paving the way for the mass production of wearable antennas integrated into clothing. The technique was verified with the fabrication and measurement of two models operating in 2.44 GHz and 868 MHz for Bluetooth low energy (BLE) and long-range (long-range) communication technologies.

Author Contributions: Conceptualization, P.A.D. and J.-Y.C.; methodology, P.A.D. and J.-Y.C.; software, P.A.D.; validation, P.A.D. and J.-Y.C.; formal analysis, P.A.D.; investigation, P.A.D.; resources, J.-Y.C.; data curation, P.A.D.; writing—original draft preparation, P.A.D.; writing—review and editing, P.A.D. and J.-Y.C.; visualization, P.A.D. and J.-Y.C.; supervision, J.-Y.C.; project administration, J.-Y.C.; funding acquisition, J.-Y.C. All authors have read and agreed to the published version of the manuscript.

Funding: This study was financially supported by Seoul National University of Science and Technology.

Institutional Review Board Statement: Not applicable.

Informed Consent Statement: Not applicable.

Data Availability Statement: Not applicable.

Conflicts of Interest: The authors declare no conflict of interest.

References

1. Mahmood, S.N.; Ishak, A.J.; Saeidi, T.; Alsariera, H.; Alani, S.; Ismail, A.; Soh, A.C. Recent Advances in Wearable Antenna Technologies: A Review. *Prog. Electromagn. Res. B* **2020**, *89*, 1–27. [CrossRef]
2. Matthews, J.C.G.; Pettitt, G. Development of flexible, wearable antennas. In Proceedings of the 3rd European Conference on Antennas and Propagation, Berlin, Germany, 23–27 March 2009; pp. 273–277.
3. Whittow, W.G.; Chauraya, A.; Vardaxoglou, J.C.; Li, Y.; Torah, R.; Yang, K.; Beeby, S.; Tudor, J. Inkjet-Printed Microstrip Patch Antennas Realized on Textile for Wearable Applications. *IEEE Antennas Wirel. Propag. Lett.* **2014**, *13*, 71–74.
4. Lee, J.H.; Dzagbletey, P.A.; Jang, M.; Chung, J.-Y.; So, J.-H. Flat Yarn Fabric Substrates for Screen-Printed Conductive Textiles. *Adv. Eng. Mater.* **2020**, *22*, 2000722. [CrossRef]
5. Bonefačić, D.; Bartolić, J. Embroidered Textile Antennas: Influence of Moisture in Communication and Sensor Applications. *Sensors* **2021**, *21*, 3988. [CrossRef] [PubMed]
6. Zhang, S.; Speight, D.; Paraskevopoulos, A.; Fonseca, D.; Luxey, C.; Whittow, W.; Pinto, J. On-body measurements of embroidered spiral antenna. In Proceedings of the Loughborough Antennas & Propagation Conference (LAPC), Loughborough, UK, 2–3 November 2015; pp. 1–5.
7. Wang, K.H.; Li, J.S. Jeans Textile Antenna for Smart Wearable Antenna. In Proceedings of the 2018 12th International Symposium on Antennas, Propagation and EM Theory (ISAPE), Hangzhou, China, 3–6 December 2018; pp. 1–3.
8. Yang, H.C.; Azeez, H.I.; Wu, C.K.; Chen, W.S. Design of a fully textile dualband patch antenna using denim fabric. In Proceedings of the 2017 IEEE International Conference on Computational Electromagnetics (ICCEM), Kumamoto, Japan, 8–10 March 2017; pp. 185–187.
9. Aprilliyani, R.; Dzagbletey, P.A.; Lee, J.H.; Jang, M.J.; So, J.-H.; Chung, J.-Y. Effects of Textile Weaving and Finishing Processes on Textile-Based Wearable Patch Antennas. *IEEE Access* **2020**, *8*, 63295–63301. [CrossRef]
10. McKerricher, G.; Titterington, D.; Shamim, A. A Fully Inkjet-Printed 3-D Honeycomb-Inspired Patch Antenna. *IEEE Antennas Wirel. Propag. Lett.* **2016**, *15*, 544–547. [CrossRef]
11. Wang, W.; Wang, Y.; Lou, S.; Zhang, S.; Zhou, Y. Effect of Ground Plane Deformation on Electrical Performance of Air Microstrip Antennas. *Int. J. Antennas Propag.* **2020**, *2020*, 4029780. [CrossRef]
12. Hong, H.; Hu, J.; Yan, X. UV Curable Conductive Ink for the Fabrication of Textile-Based Conductive Circuits and Wearable UHF RFID Tags. *ACS Appl. Mater. Interfaces* **2019**, *11*, 27318–27326. [CrossRef] [PubMed]
13. Wang, Y.; Zhang, W.; Ren, H.; Huang, Z.; Geng, F.; Li, Y.; Zhu, Z. An Analytical Model for the Tension-Shear Coupling of Woven Fabrics with Different Weave Patterns under Large Shear Deformation. *Appl. Sci.* **2020**, *10*, 1551. [CrossRef]
14. Sayem, A.S.M.; Teay, S.H.; Shahariar, H.; Fink, P.L.; Albarbar, A. Review on Smart Electro-Clothing Systems (SeCSs). *Sensors* **2020**, *20*, 587. [CrossRef] [PubMed]

15. Henkel Adhensive Technologies. Loctite Edag 479SS E&C. In *Technical Data Sheet*. 2014. Available online: https://www.gluespec.com/Materials/SpecSheet/4c2af947-bbc3-4942-8546-e3968e2655d5 (accessed on 27 January 2023).
16. ANSYS Inc. *Electronics Desktop 2021 R2: High Frequency Structure Simulator (HFSS)*; ANSYS Inc.: Canonsburg, PA, USA, 2021.
17. Balanis, C.A. *Antenna Theory: Analysis and Design*, 4th ed.; John Wiley & Sons, Inc.: Hoboken, NJ, USA, 2016.
18. Mateprincs. *Screen Ink SCAG-003 Datasheet*. 2008. Available online: http://mateprincs.com/wp-content/uploads/2021/02/SCAG-003.pdf (accessed on 27 January 2023).
19. Paraskevopoulos, A.; Fonseca, D.D.S.; Seager, R.D.; Whittow, W.G.; Vardaxoglou, J.C.; Alexandridis, A.A. Higher-mode textile patch antenna with embroidered vias for on-body communication. *IET Microw. Antennas Propag.* **2016**, *10*, 802–807. [CrossRef]
20. Zhang, J.; Yan, S.; Vandenbosch, G.A.E. A Miniature Feeding Network for Aperture-Coupled Wearable Antennas. *IEEE Trans. Antennas Propag.* **2017**, *65*, 2650–2654. [CrossRef]
21. Gupta, V.K.; Gupta, A. Design of an aperture coupled MIMO antenna for on-body communication and performance enhancement with dielectric back reflector. *Frequenz* **2021**, *75*, 61–70. [CrossRef]
22. Hertleer, C.; Tronquo, A.; Rogier, H.; Vallozzi, L.; Van Langenhove, L. Aperture-Coupled Patch Antenna for Integration Into Wearable Textile Systems. *IEEE Antennas Wirel. Propag. Lett.* **2007**, *6*, 392–395. [CrossRef]
23. Nitto Inc. P-422 NAT PTFE Film Tape. In *Product Data Sheet*. 2020. Available online: https://www.nitto.com/jp/ja/others/products/file/datasheet/PDS_NA_2Mil_PTFE_Film_Tape_P-422_012020_EN.pdf (accessed on 27 January 2023).
24. Gupta, A.; Kansal, A.; Chawla, P. Design of a wideband patch antenna and performance enhancement using an AMC reflector surface for on-body communication at 2.45 GHz. *Int. J. Electron.* **2022**, 1–16. [CrossRef]